doi: 10.22564/rbgf.v7i2.1079

Revista Brasileira de Geofísica; 1989, Vol. 7 (2), 117-127

SEISMIC REFLECTION TOMOGRAPHY *

P. HUBRAL[1]

Like in medicine or non-destructive testing, tomography has now become a well established imaging tool. In reflection seismology it is used to image the velocity or the reflectivity of the earth particularly in surface, reservoir, borehole, and crosshole seismology. Originally based on ray theory it can now be developed from the wave equation as described by Huygen's principle given in form of Kirchhoff's integral for acoustic and elastic media. Tomography thus has undergone a similar transition as seismic migration theory and both theories in fact very much relate to each other. Accepting the Born approximation for the medium to be imaged one can formulate the tomographic imaging approach as a consistent and comprehensive theory of linearized inversion. This incorporates such methods as transmission and reflection tomography for arbitrary frequencies as well as high-frequency computerized tomography that involves the Radon transform. The general framework of linearized scalar diffraction tomography will be discussed from first principles. Emphasis is put on reflection tomography. The case of zero-offset reflection tomography is treated for a Born scatterer as well as for a layered medium with reflectors buried into an arbitrary inhomogeneous velocity field.

TOMOGRAFIA DE SÍSMICA DE REFLEXÃO – Como em medicina ou testes não destrutivos, a tomografia se tornou uma técnica de imageamento bem estabelecida. Em sísmica de reflexão, ela é usada para mapear a velocidade ou reflectividade da terra principalmente em sísmica de superfície, reservatório, "furo" e "crosshole". Originalmente baseada na teoria de raio, ela pode ser desenvolvida das equações de onda como descrito pelo princípio de Huygens dado na forma da integral de Kirchhoff para meios acústicos e elásticos. Assim, a tomografia passou por uma transição similar à da migração sísmica, as duas teorias se relacionando bastante uma com a outra. Aceitando a aproximação de Born para o meio a ser mapeado, pode-se formular a tomografia como uma teoria consistente e abrangente de inversão linearizada. Isto incorpora os métodos como tomografia de transmissão e de reflexão para freqüências arbitrárias assim como a tomografia computadorizada de alta freqüência que envolve a transformada de Radon. A estrutura geral da tomografia de difração escalar linearizada será discutida de princípios básicos. Ênfase é dada à tomografia de reflexão. O caso de tomografia de reflexão de deslocamento zero é tratado para um espalhador Born assim como para um meio constituído de camadas com refletores imersos em um campo arbitrário de velocidades não homogêneas.

INTRODUCTION

Seismic Tomography has already become a widely investigated area of research. Hence only certain aspects will be summarized here. In principle one can subdivide Seismic Tomography into two main topics: Traveltime Tomography and Diffraction Tomography. Both are based on linearisation principles. In the first case the linearisation principle is based on the eiconal equation (Nolet, 1987). In the second case it is based on the wave equation (Langenberg, 1987).

Traveltime Tomography can further be divided into transmission-, reflection- and refraction tomography. These in turn can be further subdivided, depending on the type of waves and measurement configurations that are employed. For instance, refraction tomography can be based on either head

* *Invited paper presented at the I Congress of the Brazilian Geophysical Society, Rio de Janeiro, November/1989.*

[1] *Geophysikaliches Institut, Universität Karlsruhe, Hertzstr. 16, 7500 Karlsruhe 21, W. Germany.*

waves (Farell & Enivena, 1984; Amorin, et al., 1987) or diving waves (Firbas, 1981; Herman, 1980).

Diffraction tomography (Langenberg, 1987; Wu & Toksöz, 1987), on the other hand, offers also different modes of application, like the reflection mode and transmission mode. These in turn find application in reflection-, VSP- and crosshole seismic tomography.

In order not to enter into too many details at the expense of sacrificing mathematical rigor and physical insight, in this paper we will only concentrate on the Reflection Mode Diffraction Tomography. This appears to be the most valuable tomographic scheme in seismic exploration. The subject is very interesting as it reveals the close interrelation between seismic tomography and seismic migration theory.

As an extension to reflection tomography for Born scatterers, a reflection mode tomographic scheme for laterally inhomogeneous velocity models will also be presented. This scheme is also refered to as a true-amplitude zero offset migration scheme (Hubral & Tygel, 1989) of the type which Newman (1989) refers to as "modified diffraction stack" and Bortfeld (1982) as "summation migration".

INVERSE SCATTERING

Transient seismic point sources create a wavefield in the elastic earth. When this hits inhomogeneities, such as layer boundaries, reflectors and diffractors, one can observe scattered waves. This information can in turn be used in geophysical exploration to locate the scattering objects.

The theory of inverse scattering is closely related to seismic migration and can be based on the Kirchhoff integral. In the following a reflection-mode zero-offset algorithm is outlined as it shows a connection between diffraction tomography and seismic migration. It gives a sound theoretical basis for the "exploding reflector model" that has been used in seismic post-stack migration for a long time, but so far without any mathematical sound foundation. The algorithm described here (Langenberg, 1987; Wenzel & Menges, 1989) can be formulated such that it can account for other measurement configurations that are encountered in seismic exploration e.g. in transmission tomography, where either the so called frequency or angular modes of illumination are employed (Devaney, 1984; Langenberg, 1987; Wu & Toksöz, 1987).

REFLECTION MODE DIFFRACTION TOMOGRAPHY

The planar recording surface S_M will be the plane $z = d$ in a cartesian coordinate (x,y,z) system (Fig. 1). The inhomogeneity to be imaged by the method of reflection tomography falls below the plane $z = d$.

Let all inhomogeneities fall into the volume V_c surrounded by the surface of the scatterer S_c. The P- and S-wave velocity within the scatterer is dependent on the location R and given by v_P (R) and v_S (R). These velocities are assumed to differ only slightly from a constant background with P- and S-wave-velocity $\bar{v}_P$ and $\bar{v}_S$, into which the source location falls. As is well known, the P- and S-wave contribution to the particle displacement vector is obtained from the scalar potential $\phi(\mathbf{R},t)$ and the vector potential $\psi(\mathbf{R},t)$ according to

$$\mathbf{u}(\mathbf{R},t) = \nabla \phi(\mathbf{R},t) + \nabla \times \psi(\mathbf{R},t) \qquad (1)$$

with ∇ being the Nabla-Operator. As is common practice in seismic imaging, we consider in the following diffraction tomographic imaging approach only the scalar potential $\phi(\mathbf{R},t)$. This satisfies for $\mathbf{R} \notin V_c$

$$\left[\Delta - \frac{1}{c_p^2}\frac{\partial^2}{\partial t^2}\right]\phi(\mathbf{R},t) = -F(t)\delta(\mathbf{R}-\mathbf{R}_o) \qquad (2)$$

and for $\mathbf{R} \in V_c$

$$\left[\Delta - \frac{1}{c_p^{(1)2}(\mathbf{R})}\frac{\partial^2}{\partial t^2}\right]\phi(\mathbf{R},t) = 0 \qquad (3)$$

$\mathbf{R}_o \in S_M$ is the source location for a point source, whose source signature is described by the time-function F(t).
With a Fourier transformation with respect to time

$$\phi(\mathbf{R},\omega) = \int_{-\infty}^{\infty} \phi(\mathbf{R},t) \exp[j\omega t]\, dt \qquad (4)$$

we can change the wave equations (2) and (3) into the following inhomogeneous Helmholz-Equations

$$(\Delta + k_p^2)\ \phi(\mathbf{R},\omega) = -F(\omega)\delta(\mathbf{R} - \mathbf{R}_o) + k_p^2\ O(\mathbf{R})\ \phi(\mathbf{R},\omega) \qquad (5)$$

where we have introduced the so called object function

$$O(\mathbf{R}) = \left[1 - \frac{k_p^{(1)2}(\mathbf{R})}{k_p^2}\right] \Gamma(\mathbf{R}) \qquad (6a)$$

with the help of the characteristic function

$$\Gamma(\mathbf{R}) = \begin{cases} 0 & , \quad \mathbf{R} \notin V_c \\ 1 & , \quad \mathbf{R} \in V_c \end{cases} \tag{6b}$$

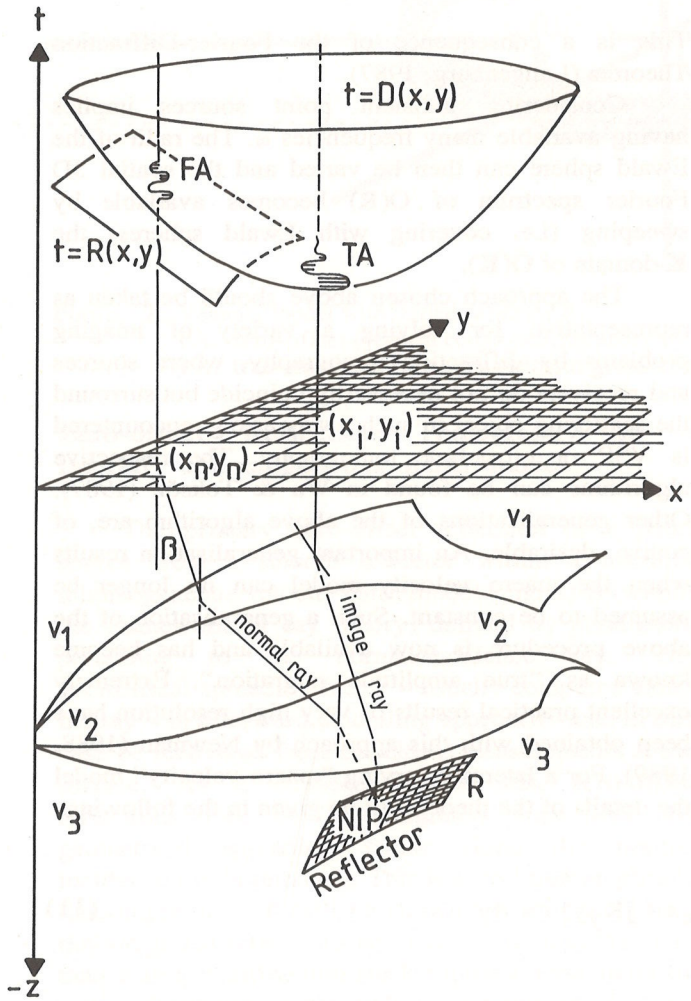

Figure 1. Constant velocity model with buried scatterer.

Ignoring the fact that the measurement-surface S_M represents a free surface, we can write the solution of equation (5) as

$$\phi(\mathbf{R},\omega) = F(\omega) \frac{\exp\,[\,jk_p\,|\mathbf{R} - \mathbf{R}_o|\,]}{4\pi\,|\mathbf{R} - \mathbf{R}_o|}$$

$$- k_p^2 \int_{-\infty}^{\infty}\int_{-\infty}^{\infty}\int_{-\infty}^{\infty} O(\mathbf{R}')\,\phi(\mathbf{R}',\omega)$$

$$\frac{\exp\,[\,jk_p\,|\mathbf{R} - \mathbf{R}'|\,]}{4\pi\,|\mathbf{R} - \mathbf{R}'|}\,d^3\,\mathbf{R}' \tag{7}$$

The first term represents the incident wavefield of the point source at $\mathbf{R}_o \in S_M$. The second term describes the scattered field of the inhomogeneities. We observe that the integral in equation (7) has the function $\phi(\mathbf{R},\omega)$ on the left-hand side and within the integral. This makes the equation in this form extremely difficult to solve for forward and inverse scattering problems. A linearisation cannot be avoided, if one wants to make use of equation (7) for tomographic imaging.

This linearisation is achieved by replacing the total field $\phi(\mathbf{R},\omega)$ in the integrand by the incident field. This replacement is justified if the velocity perturbation $v_P(\mathbf{R})-\bar{v}_R$ is sufficiently small, i.e. if the inhomogeneous velocity distribution satisfies the so called first Born approximation.

ZERO-OFFSET PROFILING

If we put $\mathbf{R}_o = \mathbf{R}$, we can write the linearized integral (7) as

$$\phi_s(\mathbf{R},\omega) = - k_p^2\, F(\omega) \int_{-\infty}^{\infty}\int_{-\infty}^{\infty}\int_{-\infty}^{\infty}$$

$$O(\mathbf{R}')\,\frac{\exp\,[2jk_p\,|\mathbf{R} - \mathbf{R}'|]}{(4\pi|\mathbf{R} - \mathbf{R}'|)^2}\,d^3\,\mathbf{R}' \tag{8}$$

Defining now a modified scattered zero-offset field according to

$$\phi_s^{mo}(\mathbf{R},\omega) = 2\pi j\,\frac{\partial}{\partial k_p}\,\frac{\phi_s(\mathbf{R},\omega)}{k_p^2\,F(\omega)} \tag{9}$$

we obtain

$$\phi_s^{mo}(\mathbf{R},\omega) = \frac{1}{4\pi} \int_{-\infty}^{\infty}\int_{-\infty}^{\infty}\int_{-\infty}^{\infty} O(\mathbf{R}') \frac{\exp[\,2jk_p|\mathbf{R}-\mathbf{R}'|\,]}{|\mathbf{R}-\mathbf{R}'|}\, d^3\mathbf{R}' \tag{10}$$

The latter equation can be inverted as it has the form of a 3D-Fourier integral.

The modification (9) involves a deconvolution of the zero-offset scattered field trace. This is described by the division with $F(\omega)$ in the squared bracket. The derivative on the other hand corresponds to "true amplitude scaling", i.e. to a multiplication of the zero-offset trace with the time t. To solve formula (10) for $O(\mathbf{R})$ is, what is generally described, an inverse source problem, where the source density is given by $O(\mathbf{R})$.

It is interesting to note that in integral (10) there appears $2\bar{k}_p$ instead of $\bar{k}_p$. This implies that the modified scattered wavefield $\phi_s^{mo}(\mathbf{R},\omega)$ is a wavefield, where the true "background-velocity" or "macro-velocity" $\bar{v}_p$ is replaced by $\bar{v}_p/2$. We observe that this replacement is well known in wave equation migration theory, when one introduces the so called "exploding reflector model".

Hence formulas (9) and (10) give a mathematical justification of the exploding reflector assumption. We note, that indeed the zero-offset traces (which in a zero-offset section do not satisfy one wave equation) can be modified to exploding reflector traces as long as the Born approximation holds true.

The inversion of integral (10) for $O(\mathbf{R})$ now solves our 3D inverse tomographic scattering problem as we can accept that the zero-offset field is given at $\mathbf{R} \in S_M$. Upon S_M we have $\mathbf{R} = (x,y,d)$. Now choosing the integration variable $\mathbf{R} = (x',y',z')$ also in cartesian coordinates, the volume integral (10) becomes a 2D convolution integral over x and y.

Taking the 2D Fourier transform of $\phi_s^{mo}(\mathbf{R},\omega)$ with respect to x and y

Equation (13) is the fast tomographic algorithm, which relates to the Stolt algorithm (Stolt, 1978).

The 2D Fourier spectrum of the modified zero-offset data with respect to x and y is proportional to the 3D spatial Fourier transform $\tilde{O}$ of the object function upon the so called Ewald-sphere

$$K_z = + \sqrt{4k_p^2 - k_x^2 - k_y^2}$$

This is a consequence of the Fourier-Diffraction Theorem (Langenberg, 1987).

Considering transient point sources implies having available many frequencies ω. The radii of the Ewald sphere can then be varied and the spatial 3D Fourier spectrum of $O(\mathbf{R})$ becomes available by sweeping (i.e. covering with Ewald spheres) the $\mathbf{K}$-domain of $\tilde{O}(\mathbf{K})$.

The approach chosen above should be taken as representative for solving a variety of imaging problems by diffraction tomography, where sources and receivers do not necessarily coincide but surround the scattering object in such a way as e.g. encountered is VSP or cross-hole tomography. The respective algorithms can be found in Wu & Toksöz (1987). Other generalisations of the above algorithm are, of course, desirable. An important generalisation results when the macro velocity model can no longer be assumed to be constant. Such a generalisation of the above procedure is now available and has become known as "true amplitude migration". Extremely excellent practical results of very high resolution have been obtained with this approach by Newman (1988, 1989). For a laterally varying "macro-velocity" model the details of the theory will be given in the following.

$$\phi_s^{mo}(K_x,K_y,z,\omega) = \int_{-\infty}^{\infty}\int_{-\infty}^{\infty} \phi_s^{mo}(x,y,z,\omega)\exp[-jK_x x - jK_y y]\,dx\,dy \tag{11}$$

we obtain

$$\phi_s^{mo}(K_x,K_y,d,\omega) = \frac{j}{2}\int_{-\infty}^{\infty} \tilde{O}(K_x,K_y,z') \frac{\exp[\,j|d-z'|\sqrt{4k_p^2 - K_x^2 - K_y^2}\,]}{\sqrt{4k_p^2 - K_x^2 - K_y^2}}\, dz' \tag{12}$$

and as $d > z'$

$$\phi_s^{mo}(K_x,K_y,d,\omega) = \frac{j}{2} \frac{\exp[\,jd\sqrt{4k_p^2 - K_x^2 - K_y^2}\,]}{\sqrt{4k_p^2 - K_x^2 - K_y^2}} \tag{13}$$

$$\tilde{O}(K_x,K_y,K_z = \sqrt{4k_p^2 - K_x^2 - K_y^2})$$

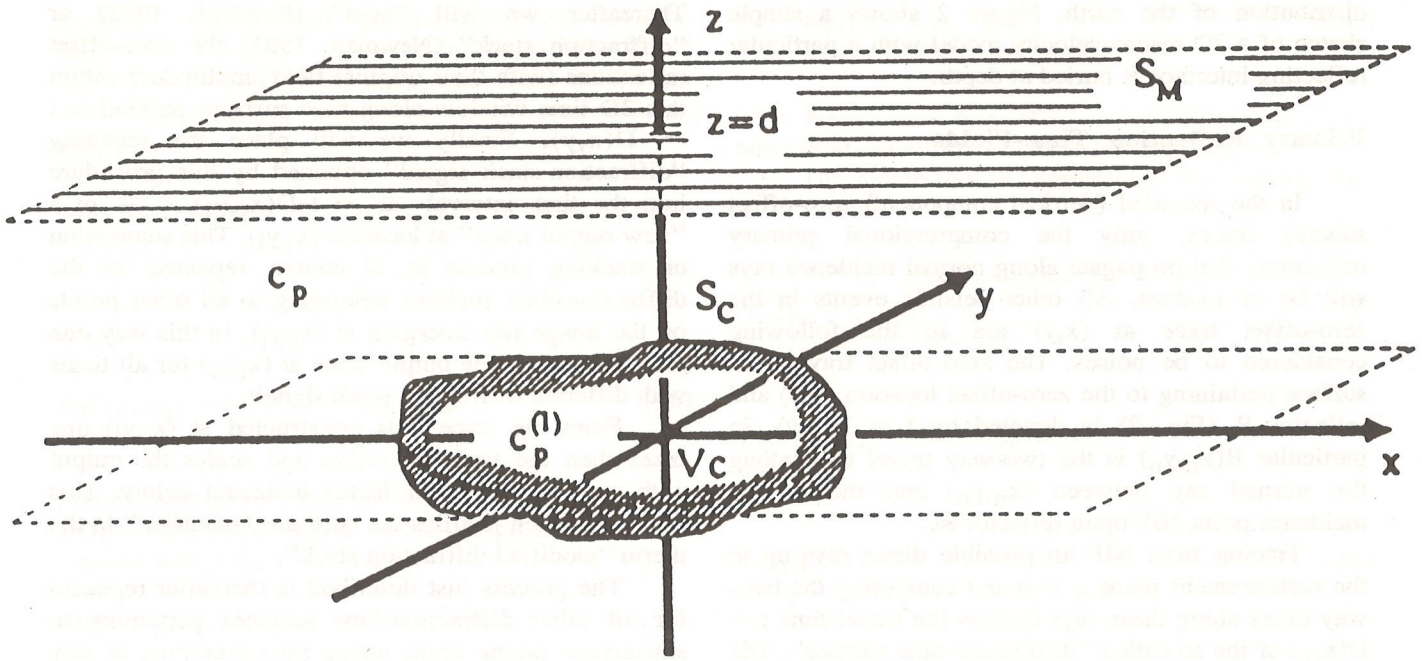

Figure 2. Velocity model with buried reflector R.
FA: zero-offset (vertical component) primary reflection (with geometrical spreading loss).
TA: true-amplitude reflection (without geometrical spreading loss).

Zero-offset Reflection Tomography in a laterally inhomogeneous earth model

The primary zero-offset reflection of a point source from a smooth reflector within a laterally inhomogeneous velocity earth model (Fig. 2) is (within the framework of ray theory) defined by parameters pertaining to the normal-incidence ray. The geometrical spreading factor – usually computed along the ray – in a forward modelling approach – can in this case be recovered from traveltime measurements at the surface. As a consequence of this, zero-offset reflections can be time-migrated such that the geometrical spreading factor along the normal incidence ray is removed. This lead to "true-amplitude time-migration". It will be shown that true-amplitude time-migrated reflections are obtained by nothing more than a simple diffraction stack followed essentially by a time derivative of the diffraction-stack traces. For a small transmission loss of a primary zero-offset reflection through the layers, the true-amplitude time-migrated reflection provides consequently a direct measure for the reflection coefficient at the reflecting lower end of the normal-incidence ray.

Basic Concepts

Let us assume the earth to be isotropic, elastic and inhomogeneous in such a way that primary zero-offset reflections can be well described by ray theory. For instance, the earth may be assumed to consist locally of arbitrarily many layers of constant P-wave and S-wave velocity and density. There may in addition be many reflectors buried within the earth with normal-incidence reflection coefficients varying laterally. The principal objective of this work is to find the (time-migrated) positions of all reflectors as well as their laterally changing normal-incidence reflection coefficients. In the pursuit of this objective, some interesting properties of normal-incidence rays will be presented below.

Measurement Configuration

Coincident shots and receivers are expected to fall upon a dense (rectangular) grid on the measurement plane z = 0 (Fig. 2). Further, let us assume that at each grid location, i.e. at the zero-offset location (x,y), one records the vertical-displacement component of the elastodynamic wavefield resulting from a compressional point source placed at the very same location. All point sources are moreover expected to have identical source signatures at all surface locations (x,y).

Macro-Velocity Model

It is assumed that the true P-wave velocity distribution in the earth is well approximated by an already available "macro-velocity model". In this model ray travel times from any subsurface point to arbitrary points, at the masurement plane z = 0, are expected to agree well with the true P-wave travel times, in the corresponding actual P-wave velocity

distribution of the earth. Figure 2 shows a simple sketch of a 3D macro-velocity model with a particular reflecting interface R buried at depth.

Primary Reflection Time-Fields

In the recorded (vertical component) zero-offset seismic traces, only the compressional primary reflections that propagate along normal incidence rays will be of interest. All other seismic events in the zero-offset trace at (x,y) are in the following considered to be noises. The zero-offset travel-time surface pertaining to the zero-offset location (x,y) and reflector R (Fig. 2) is denoted by $t = R(x,y)$. In particular $R(x_n,y_n)$ is the two-way travel time along the normal ray between (x_n,y_n) and the normal incidence point NIP upon reflector R.

Tracing from NIP all possible direct rays up to the measurement plane $z = 0$ and computing the two-way times along these rays defines the travel-time $t = D(x,y)$ of the so called "diffraction-time surface". The minimum time of this surface is $D(x_i,y_i)$, with (x_i,y_i) being the surface location of the image ray (Hubral, 1977) to NIP. While the normal-incidence ray is perpendicular to the reflector, the image ray is perpendicular to the measurement plane. It is obvious that D(x,y) is tangent to R(x,y) at (x_n,y_n).

Though the time surface D(x,y) is identical with the one that would be observed in the zero-offset data for a diffractor at NIP, we will in the following theoretical treatment not permit any such diffractors on the reflecting interfaces.

Modified Diffraction Stack

Let us assume that, for each subsurface point within the available macro-velocity model, one has constructed the corresponding diffraction-time surface. In particular, let us consider all point on the image ray through (x_i,y_i). The diffraction-time surfaces pertaining to these points have all their apex at (x_i,y_i).

Many of these diffraction-time surface will be tangent to certain primary reflection-time surfaces that are present in the zero-offset recording. These will pertain to various subsurface reflectors intersected by the image ray. The aperture of each diffraction time surface should, of course, be chosen such that all (unknown) reflection time surfaces in the zero-offset recording, which pertain to subsurface reflectors crossed by the image ray through (x_i,y_i), will fall into the selected aperture range.

Below we will choose a 3D-time window parallel to the diffraction-time surface $t = D(x,y)$ such that D(x,y) will be at its center. In other words we will choose the time window $-\in < t - D(x,y) < \in$, where $\in$ has to be chosen such that seismic pulses from reflector R fully fall into the time window. Thereafter we will "sum" (Bortfeld, 1982) or "diffraction stack" (Newman, 1985) the zero-offset reflections (with their original field amplitudes) within this 3D time window along time surfaces parallel to $t = D(x,y)$. Finally we will place the resulting "diffraction-stack signal" obtained by this procedure into the time interval $-\in < t-D(x_i,y_i) < \in$ of a "new output trace" at location (x_i,y_i). This summation or stacking process is, of course, repeated for the diffraction-time surfaces belonging to all other points on the image ray emerging at (x_i,y_i). In this way one can fill up the new output trace at (x_i,y_i) for all times with different diffraction stack signals.

From the trace thus constructed at (x_i,y_i) one takes then the time derivative and scales the output with a certain constant factor indicated below. This latter operation justifies the attribute "modified" in the therm "modified diffraction stack".

The process just described is thereafter repeated for all other diffraction-time surfaces pertaining to subsurface points upon image rays emerging at any other possible surface location.

True Amplitude Time-Migration

As a result of the above "modified diffraction stack" one obtains so called "true-amplitude time-migrated 3D data" in the (x,y,t) domain of Figure 2. That this is indeed the case will be shown below, where we will prove that the procedure outlined above will indeed remove from zero-offset primary reflections their geometrical spreading loss along normal rays, when "time-migrating" these reflection from the time surface R(x,y) to the time-migrated surface I(x,y) (not shown in Figure 2). The zero-offset reflection FA in Figure 2 will thus be time-migrated to the true-amplitude reflection TA.

I(x,y) is the two-way time along image rays connecting the surface location (x,y) with reflector R. I(x,y) can consequently be viewed as the time-surface defined by all the minima of the diffraction-time surfaces pertaining to points on reflector R.

We note that image rays would make it possible to "depth-migrate" (Hubral, 1977) the time surface I(x,y) into the unknown reflector R at depth. In the following however, we will only perform the modified diffraction stack on the zero-offset (x,y,t) data volume, i.e. we will present the theory for a true-amplitude "time migration" and not for a true-amplitude "depth migration". Of course, it is well know that the macro-velocity model for a depth migration should in general be more precise than that for a time migration.

RAY THEORY FOR NORMAL INCIDENCE REFLECTIONS

For a compressional point source and receiver at

location (x_n,y_n) the vertical-component of the displacement vector of the primary compressional reflection can (within the framework of ray theory and if we ignore the free surface) be expressed as (Hubral, 1983):

$$u(x_n,y_n,z=0,t) = \mathrm{Re}\{u_o(x_n,y_n)\, W(t - R(x_n,y_n))\}\ , \tag{14}$$

where

$$u_o(x_n,y_n) = \frac{1}{L}\, K_r\, (\Pi\, K_t)\, \cos\beta \tag{15}$$

β is the emergence angle of the normal ray at (x_n,y_n). W(t) is the analytic signal of the compressional source wavelet w(t), i.e.,

$$W(t) = w(t) - iH\,[w(t)] \tag{16}$$

H denotes the Hilbert transform

$$H\,[w(t)] = \frac{1}{\pi}\, PV \int_{-\infty}^{\infty} \frac{w(\tau)}{t-\tau}\, d\tau \tag{17}$$

$K_r = K_r(x_n,y_n)$ is the (real) normal-incidence reflection coefficient at NIP. This may vary as a function of (x_n,y_n). $((\Pi K_t) = \Pi K_t(x_n,y_n))$ is the product of all the (real) transmission coefficients encountered by the primary compressional wave on its two-way path along the normal incidence ray from (x_n,y_n) to NIP and back. It will be a positive quantity often close to unity.

Geometrical Spreading

L is the geometrical spreading factor in formula (15) which, in a forward modelling approach, would, in general, be computed by dynamic ray tracing (Cerveny, 1977) along the normal incidence ray. Such a computation is, however, not required in the following procedure.

With respect to the normal ray the factor L is given by the expression (Hubral, 1983; Krey, 1983):

$$L = \frac{2}{\sqrt{Q_A}}\ , \tag{18}$$

where

$$Q_A = \det A \tag{19a}$$

and

$$A = K_{NIP} - K_N\ , \tag{19b}$$

with K_{NIP} and K_N being two fundamental 2 x 2 wavefront curvature matrices specified below.

The square root in expression (18) is defined by

$$\sqrt{Q_A} = \begin{cases} \sqrt{|Q_A|}\ \mathrm{sgn}(\mathrm{tr}A) & Q_A > 0 \\ i\sqrt{|Q_A|} & Q_A < 0 \end{cases} \tag{20}$$

with the sign-function given as

$$\mathrm{sgn}(x) = \begin{cases} -1 & , x < 0 \\ +1 & , x > 0 \end{cases} \tag{21}$$

trA denotes the trace of the matrix A. Note that the solution (14) is invalid if Q_A is zero.

K_{NIP} and K_N relate to the two-way time surfaces $t = R(x,y)$ and $t = D(x,y)$ as follows (Bortfeld, 1989):

$$K_N = K_N(x_n,y_n) = \frac{V_1}{2\cos^2\beta} \begin{bmatrix} \frac{\partial^2 R(x,y)}{\partial x^2} & \frac{\partial^2 R(x,y)}{\partial x\, \partial y} \\ \frac{\partial^2 R(x,y)}{\partial x\, \partial y} & \frac{\partial^2 R(x,y)}{\partial y^2} \end{bmatrix} \tag{22a}$$

$$K_{NIP} = K_{NIP}(x_n,y_n) = \frac{V_1}{2\cos^2\beta} \begin{bmatrix} \frac{\partial^2 D(x,y)}{\partial x^2} & \frac{\partial^2 D(x,y)}{\partial x\, \partial y} \\ \frac{\partial^2 D(x,y)}{\partial x\, \partial y} & \frac{\partial^2 D(x,y)}{\partial y^2} \end{bmatrix} \tag{22b}$$

where all derivatives are taken at (x_n,y_n). v_1 is the compressional near-surface velocity, which is assumed to be known.

The wavefront curvature matrices K_{NIP} and K_N can be associated with two hypothetical waves. K_{NIP} (x_n,y_n) can be viewed as pertaining to the wavefront emerging at (x_n,y_n), which has its origin in a hypothetical point-source at NIP. K_N (x_n,y_n), on the other hand, can be viewed as pertaining to the wavefront emerging at (x_n,y_n) which has its origin in a hypothetical wave originating at all points of R simultaneously. Alternatively one can view K_{NIP} and K_N as pertaining to two "eigenwaves", which have the unique property that, when propagating down and up the normal incidence ray, they start and emerge at the surface with the same wavefront (Hubral, 1983).

The definition (20) of the square root in formula (18) has some interesting consequences concerning solution (14). Provided that the velocity above the reflector is constant and the reflection coefficient K_r (x_n,y_n) at NIP is positive, the reflected zero-offset pulse at (x_n,y_n) may either have the shape w(t), -w(t) or H[w(t)].

It is well known that the reflected pulse shape depends on the number of caustics along the normal ray, which are usually counted in forward ray modelling. In order to guarantee a correct true amplitude recovery of the source pulse, we assume that no caustics exist in a laterally inhomogeneous medium.

As indicated above, no CMP data nor any traveltimes for interpreted reflections are required for the theory described here. However, with the recorded 3D zero-offset data also the macro-velocity model is expected to be given. This implicitly defines consequently the time-surface D(x,y) and the curvature matrix K_{NIP} (x_n,y_n), thus making the computation of the spreading factor L at any location (x_n,y_n) possible without identifying primary reflections from reflector R nor tracing a normal ray to it. We will not enter here into a discussion concerning the computation of the macro-velocity model. This surely cannot be derived from the zero-offset data but requires borehole or CMP measurements.

THEORY OF MODIFIED DIFFRACTION STACK MIGRATION

We now provide a mathematical formulation of the summation method, which we prefer to call "modified diffraction stack". For simplicity we make use of analytic signals, i.e. operate with the complex version of the vertical-component of the displacement vector of the compressional primary reflection recorded at (x_n,y_n). This is given as the expression within the parenthesis of formula (14)

$$U(x_n, y_n, t) = u_o (x_n, y_n)\, W(t - R (x_n, y_n)) \tag{23}$$

Diffraction Stack

With respect to the zero-offset location (x_n,y_n) we define

$$g(x,y) = D(x,y) - R(x,y) \tag{24}$$

We know that in the vicinity of (x_n,y_n) we have

$$g(x,y) \simeq \frac{1}{2} [x - x_n, y - y_n]\, \tilde{A}\, [x - x_n, y - y_n]^T \tag{25}$$

where T denotes the transpose and

$$\tilde{A} = (K_{NIP} - K_N) \frac{2\cos^2\beta}{v_1} = A \frac{2\cos^2\beta}{v_1} \tag{26}$$

Formula (25) results because

$$g(x_n, y_n) = \nabla g(x_n, y_n) = 0 \tag{27}$$

For a rectangle

$$M_n \equiv \{ (x,y) \mid |x - x_n| < \epsilon_1, |y - y_n| < \epsilon_2 \} \tag{28}$$

centred at (x_n,y_n) let us consider the following integral to be representative for a "diffraction stack" for the zero-offset reflections from reflector R in rectangle M_n.

$$U_i (x_n,y_n,\tau) = \iint_{M_n} dx\, dy\, U(x,y,\tau + D(x,y))$$

$$= \iint_{M_n} dx\, dy\, u_o (x,y)\, W(\tau + D(x,y) - R(x,y))$$

$$= \iint_{M_n} dx\, dy\, u_o (x,y)\, W(\tau + g (x,y)) \tag{29}$$

The index i indicates that the resulting "diffraction-stack signal" obtained by the right-hand side expression is to be transferred into the apex of the diffraction-time-surface D(x,y) at the output trace at location (x_i,y_i). The arguments x_n, y_n, on the other hand, in the left-hand side of formula (29) should be taken as an indication that the integral (29) will get its main contribution from the zero-offset reflections in the vicinity of (x_n,y_n). Though we allow that τ in integral (29) may take on any value, we remark that in the discrete implementation of formula (29) only a

finite range of values for τ needs to be considered. This we already indicated above, when we shortly summarized the modified diffraction stack. In this connection it should also be made clear that in the practical implementation of the algorithm, we will use instead of M_n the interior of a sufficiently large circle centered at (x_i,y_i) as we assume no a priori knowledge with respect to the point of tangency of R(x,y) and D(x,y).

The τ-Fourier transform of the above expression (29) can be written

$$U_i\,(x_n,y_n,\omega) = \hat{W}(\omega) \iint_{M_n} dx\,dy\; u_o\,(x,y)\,\exp\,[i\omega\, g(x,y)] \qquad (30)$$

Where we have used the notation

$$\hat{W}(\omega) = \int_{-\infty}^{\infty} d\tau\,\exp\,[-i\omega\tau]\,W(\tau) \qquad (31)$$

We also have interchanged the order of space and time integration and used the shifting property of the Fourier transform. The integral in (30) is of the form studied by Hubral & Tygel (1989). It shows that, for large positive $\omega >> 1$,

$$\hat{U}_i\,(x_n,y_n,\omega) \simeq \hat{W}(\omega)\,u_o\,(x_n,y_n)\,\frac{1}{\sqrt{Q_A}}\,\left[\frac{2\pi i}{\omega}\right]\,, \quad (\omega > 0) \qquad (32)$$

with

$$\hat{U}_i\,(x_n,y_n,\omega) = \overline{U_i\,(x_n,y_n,-\omega)}\,, \quad (\omega < 0) \qquad (33a)$$

and

$$Q_A = \det \tilde{A} \qquad (33b)$$

Also the square root in equation (32) turns out to be

$$\sqrt{Q_A} = \cos\beta\,\sqrt{2/v_1}\,\sqrt{Q_A} = \cos\beta\,\sqrt{2/v_1}\,\frac{2}{L} \qquad (34)$$

with the root of Q_A being defined in expression (20). L, as one observes, is the geometric spreading factor of the zero-offset reflection at (x_n,y_n). Substituting equation (34) into formula (32), one finds for $\omega >> 1$

$$\hat{U}_i\,(x_n,y_n,\omega) \simeq \hat{W}(\omega)\,u_o\,(x_n,y_n)\,\sqrt{v_1/2}\,\frac{L}{2}\,\frac{1}{\cos\beta}\,\left[\frac{2\pi}{\omega}\,i\right]\,, \quad (\omega > 0) \qquad (35)$$

Substituting the expression (15) for $u_o\,(x_n,y_n)$ yields

$$\hat{U}_i(x_n,y_n,\omega) \simeq \hat{W}(\omega)\,\left[K_r(\Pi K_t)\,\frac{1}{L}\,\cos\beta\right]\,\left[\sqrt{v_1/2}\,\frac{L}{\cos\beta}\,\left[\frac{\pi}{\omega}\,i\right]\right] \qquad (36)$$

$$= \hat{W}(\omega\,K_r(\Pi\,K_t)\,\sqrt{v_1/2}\,\left[\frac{\pi}{\omega}\,i\right]\,, \quad (\omega > 0)$$

or

$$K_r(\Pi\,K_t)\,\sqrt{v_1/2}\,\hat{W}(\omega) = \left[\frac{-i\omega}{\pi}\right]\,\hat{U}_i\,(x_n,y_n,\omega)\,, \quad (\omega > 0) \qquad (37)$$

The Fourier transform pair for analytic signals F(t) is

$$F(t) = \frac{1}{2\pi}\int_o^{\infty} d\omega\,\exp\,[i\omega t]\,\hat{F}\,(\omega) \qquad (38a)$$

$$\hat{F}\,(\omega) = \int_{-\infty}^{\infty} dt\,\exp\,[-i\omega t]\,F(t) \qquad (38b)$$

Indicating this relationship by $\hat{F}(\omega) \leftrightarrow F(t)$, one notes that

$$\left[\frac{-i\omega}{\pi}\right]\,\hat{U}_i\,(x_n,y_n,\omega) \leftrightarrow -\frac{d}{dt}\,\left[\frac{1}{\pi}\,U_i\,(x_n,y_n,t)\right] \qquad (39)$$

Hence one finds

$$K_r\,(\Pi\,K_t)\,\sqrt{v_1/2}\,W(t) \simeq -\frac{1}{\pi}\,\frac{d}{dt}\,U_i\,(x_n,y_n,t) \qquad (40)$$

or taking real parts

$$K_r\,(\Pi\,K_t)\,\sqrt{v_1/2}\,w(t) \simeq -\frac{1}{\pi}\,\frac{d}{dt}\,u_i\,(x_n,y_n,t) \qquad (41)$$

where $u_i = \mathrm{Re}\,U_i$.

Introducing the definition $w_{ta}(t)$ for the true amplitude signal

$$K_r(\Pi K_t)\, w(t) = w_{ta}(t) \qquad (42)$$

one obtain the final result

$$w_{ta}(t) \sim \frac{1}{\pi \sqrt{v_1/2}} \frac{d}{dt} [u_i (x_n, y_n, t)] \qquad (43)$$

where

$$u_i (x_n, y_n, t) = \iint_{M_r} dx\, dy\, u(x,y,t + D(x,y)) \qquad (44)$$

It is interesting to observe that in a true-amplitude trace (42) there appears only the source pulse w(t), even though the zero-offset reflections could have been pulses of the form -w(t) and H[w(t)], due to caustics encountered along the normal ray. As the above theory shows, the modified diffraction stack migration removes the geometrical spreading loss in the time-migration of the reflections. It also reconstitutes the original source pulse w(t) in the case of a constant background velocity model. This very much helps the interpretation as the sign of K_r is also correctly recovered. In the case of caustics on normal rays in a laterally inhomogeneous velocity medium the correct source pulse need however not be correctly reconstituted by the above procedure.

CONCLUSIONS

Rather than having entered into the broad general subject of tomography, we treated only one aspect in some rather detail, namely the reflection mode diffraction tomography for zero-offset recordings. We first treated the case of a Born-type scatterer. Thereafter we extended the method to a laterally inhomogeneous model. In a laterally inhomogeneous earth, where compressional zero-offset reflections from smoooth subsurface reflectors are well approximated by ray theory, one can construct so-called "true-amplitude-time-migrated" reflections by nothing more than a diffraction stack, followed by a scaled time derivation of the resulting stack trace. To make this migration method operationally efficient one has to implement (a) a very quick ray tracing from the various subsurface points of the macro-velocity model to the measurement surface and (b) a very fast traveltime interpolation in order to obtain all the diffraction time surfaces required for the stack. Very efficient algorithms, for achieving such goals exist (Goldin, 1986).

Of course, in cases with a small lateral change of velocity the RMS-velocity may often be good enough to define the diffraction time surfaces. Then there is no need for any ray tracing at all.

An important aspect, of course, is the performance of the presented migration method in the presence of random noise. Here first computational experiments (Mürz, 1985; Krey, 1987) show that the modified diffraction stack favourably enhances the signal-noise ratio, just as one would expect from any stacking process.

REFERENCES

AMORIN, W.N. de; HUBRAL, P. & TYGEL, M. – 1987 – Computing field statics with the help of seismic tomograhy. Geophys. Prospecting, **35**: 907-919.

BORTFELD, R.K. – 1982 – Phaenomene und Probleme beim Modellieren und Invertieren. In Modellverfahren bei der Interpretation Seismischer Daten: DUGI, Fachausschuss, Geophysik, Celle.

BORTFELD, R.K. – 1989 – Geometrical ray theory, rays and travel-times in seismic systems (second-order approximation of the traveltimes). Geophysics, **54**: 342-349.

CERVENY, V. et al. – 1977 – Ray method in seismology. Praha.

DEVANEY, A.J. – 1984 – Geophysical diffraction tomography. IEEE Trans. Geosc. Rem. Sens. Ge-22, 3-13.

FARRELL, R.C. & ENIVENA, R.N. – 1984 – Surface consistent decomposition of refraction ray paths. Presented at the 54th Ann. International Meeting Soc. Expl. Geophysic, Atlanta, USA.

FIRBAS, P. – 1981 – Inversion of travel-time data for laterally heterogeneous velocity structure-linearisation approach. Geophys. J.R. astr. Soc., **67**: 189-198.

GOLDIN, S.V. – 1986 – Seismic traveltime inversion. SEG monograph.

HERMAN, G.T. – 1980 – Image reconstruction from projections - the fundamentals of computerized tomography. Academic Press, 316 p.

HUBRAL, P. – 1977 – Time-migration - some ray theoretical aspects. Geophys. Prosp., **25**: 738-745.

HUBRAL, P. – 1983 – Computing true amplitude reflections in a laterally inhomogeneous earth. Geophysics, **48**: 1051-1062.

HUBRAL, P. & TYGEL, M. – 1989 – True-amplitude zero offset migration. Submitted to Geophysics.

KREY, Th. – 1983 – A short and straightforward derivation of two equations from Hubral's paper. "Computing true amplitude reflections in a laterally inhomogeneous earth". Geophysics, **48**: 1129-1131.

KREY, Th. – 1987 – Attenuation of random noise by 2D and 3D CDP - Stacking and Kirchhoff Migration. Geophys. Prosp., **35**: 135-147.

LANGENBERG, K.J. – 1987 – Applied inverse problems for acoustic, electromagnetic and elastic wave scattering. In Basic Methods of Tomography and Inverse Problems. Eds. P.C. Sabatier, Malvern Press, Adam Hilger, Bristol and Philadelphia.

MÜRZ, M. – 1985 – Amplitudenuntersuchung bei Migrationsverfahren. Diplomarbeit, Institut für Geophysik der Technischen Universität Clausthal.

NEWMAN, P. – 1985 – Short-offset 3D: a case history. Paper presented at the 47th EAEG Meeting, Budapest.

NEWMAN, P. – 1988 – Cost effective 3D seismic survey during a north sea winter. SEG Meeting, Anaheim,

California.

NEWMAN, P. – 1989 – Short offset 3D marine seismic applications. 51st EAEG Meeting, Berlin.

NOLET, G. – 1987 – Seismic tomography - with applications. In Global Seismology and Exploration Geophysics. D. Reidel Publ. Co.

STOLT, R.H. – 1978 – Migration by Fourier transformation. Geophysics, 43: 23-48.

WENZEL, F. & MENGES, D. – 1989 – A comparison between Born inversions and frequency-wavenumber migration. Geophysics, 54: 1006-1011.

WU, R.S. & TOKSÖZ, M.N. – 1987 – Diffraction tomography and multisource holography applied to seismic imaging. Geophysics, 52: 11-25.

Versão original recebida em Nov/89
Versão final em Dez/89
E.A.: M.S.A.